Journal of Sound and Vibration (1997) **202**(3), 427–437

LETTERS TO THE EDITOR

STABILITY ANALYSIS OF A ROTATING BEAM UNDER A MOVING MOTION-DEPENDENT FORCE

Y.-M. Huang and K.-K. Chang

Department of Mechanical Engineering, National Central University, Chung-Li, Taiwan 320, *Republic of China*

(*Received* 1 *June* 1994, *and in final form* 29 *July* 1996)

1. INTRODUCTION

This letter is concerned with the stability of a rotating beam subject to a motion-dependent moving force. The model is chosen for study of the vibration of the workpiece in the lathing process. Interactions of rotation, force motion and motion-dependence are particularly discussed.

Papers related to the current research are as follows. Kenney [1] derived the formulation of the critical moving speed of the load on a beam on an elastic foundation. Florece [2] solved the problem of the dynamic behavior of a beam excited by a constant moving force. The stability and response of a non-rotating beam acted on by a motion-dependent force moving at a constant speed was discussed comprehensively by Katz *et al*. [3]. Their results showed the increase of stiffness of the beam due to the motion-dependent external force. Lee *et al*. [4] studied the vibration problem of a rotating beam subject to a constant moving load via the method of modal analysis. Katz *et al*. [5] further published a paper about the dynamic response of a rotating beam subject to a constant moving force at a constant speed. They showed the induction of the deflection perpendicular to the load direction due to the effect of rotation. Huang and Chen [6] solved the problem of a spinning orthotropic beam excited by a moving harmonic load. Argento *et al*. [7–10] have also presented a series of papers related to the present topic. Their results were, however, primarily based on a numerical scheme. The authors here explore the stability phenomenon from an analytic approach and eventually verify the approach with numerical solutions.

A rotating Rayleigh beam model is used in this paper. Compared to an Euler beam, the Rayleigh beam formulation contains additional rotary inertia terms. The reason for including the rotary inertia of the shaft is that the inertia, subsequently the gyroscopic effect as well, becomes significant at high rotation frequencies.

2. EQUATIONS OF MOTION

A slender beam of length l and cross-section A, is shown in Figure 1. $V(x, t)$ and $W(x, t)$ are the absolute displacements in the inertia co-ordinates xyz. The beam is rotating about the x-axis at a constant frequency Ω. Via Hamilton's principle, the equations of motion of the rotating beam are obtained as [11]

$$\frac{\partial V^{*4}}{\partial^4 x^*} + \frac{\partial V^{*2}}{\partial^2 t^*} - r^{*2}\frac{\partial V^{*4}}{\partial^2 x^* \partial^2 t^*} - 2r^{*2}\Omega^*\beta_1^{*2}\frac{\partial W^{*3}}{\partial^2 x^* \partial t^*} + 2r^{*2}\Omega^{*2}\beta_1^{*4}\frac{\partial V^{*2}}{\partial^2 x^*} = p_y^*,$$

$$\frac{\partial W^{*4}}{\partial^4 x^*} + \frac{\partial W^{*2}}{\partial^2 t^*} - r^{*2}\frac{\partial W^{*4}}{\partial^2 x^* \partial^2 t^*} + 2r^{*2}\Omega^*\beta_1^{*2}\frac{\partial V^{*3}}{\partial^2 x^* \partial t^*} + 2r^{*2}\Omega^{*2}\beta_1^{*4}\frac{\partial W^{*2}}{\partial^2 x^*} = p_z^*. \quad (2)$$

In equations (1) dimensionless parameters are defined for simplicity as

0022–460X/97/180427 + 11 $25.00/0/SV 960741

$$V^* = V/l, \qquad W^* = W/l, \qquad r^* = \sqrt{I/A}/l, \qquad \Omega^* = \Omega/(\beta_1^2\sqrt{EI/\rho A}),$$
$$x^* = x/l, \qquad t^* = (\sqrt{EI/\rho A}/l^2)t, \qquad p_y^* = (l^3/EI)p_y, \quad p_z^* = (l^3/EI)p_z, \tag{2}$$

where ρ, E, p_y and p_z are the mass density, Young's modulus, and force magnitudes, respectively. The beam is assumed to be symmetric: i.e., $I_y = I_z = I$. In equations (1) and (2), r^* is equivalent to the slenderness ratio of the beam, β_m ($m = 1, 2, \ldots$) denotes the mth eigenvalue of the non-rotating Euler beam, and is related to its mth natural frequency ω_{Em} by $\beta_m^2 = \omega_{Em}\sqrt{\rho A/EI}$. Furthermore, the corresponding dimensionless eigenvalue is defined as $\beta_1^* = \beta_1 l$.

The partial differential equations (1) can be further discretized via Galerkin's method. Let

$$V^* = \sum_{m=1}^{N} \zeta_m(t^*)X_m(x^*), \qquad W^* = \sum_{m=1}^{N} \eta_m(t^*)X_m(x^*), \tag{3}$$

where $\zeta_m(t^*)$ and $\eta_m(t^*)$ are two generalized co-ordinates associated with the mth trial mode $X_m(x^*)$, and N is the number of modes deemed necessary for satisfactory convergence. A reasonable choice of the $X_m(x^*)$ set is that of the modes of the corresponding non-rotating Euler beam.

The external force considered here moves along the axial direction of the beam at a constant speed v. Thus, the non-dimensional force can be expressed as

$$p_y^*(x^*, t^*) = \hat{p}_y^*\,\delta(x^* - (l_c^*/2\pi)\beta_1^{*2}v^*t^*),$$
$$p_z^*(x^*, t^*) = \hat{p}_z^*\,\delta(x^* - (l_c^*/2\pi)\beta_1^{*2}v^*t^*), \tag{4}$$

where $\hat{p}_y^*$ and $\hat{p}_z^*$ are the force magnitudes, and the dimensionless characteristic length, of mode $X_1(x^*)$, is denoted as $l_c^* = l_c/l$ with l_c wavelength of the first mode shape. The non-dimensional speed of the external force is defined as $v^* = v/v_{Ecr}$ with $v_{Ecr} = (\beta_1^2 l_c/2\pi)\sqrt{EI/\rho A}$ the critical speed of a non-rotating Euler beam [1].

The motion-dependent force components are functions of the displacement,

$$\hat{p}_y^* = P_y^* - \gamma V^*, \qquad \hat{p}_z^* = P_z^*, \tag{5}$$

with γ a constant. The displacement W^* as well as the force in the z direction was found to only affect slightly the dynamic behavior of the rotating beam [12]; therefore, the dependence of the force $\hat{p}_y^*$ on W^* is ignored and $\hat{p}_z^*$ is assumed to be a constant.

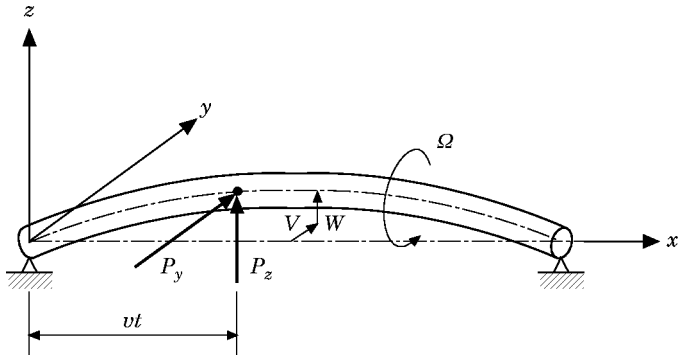

Figure 1. The rotating beam.

The two ends of the beam are taken to be simply supported herein. The equations of motion derived, nevertheless, are suitable for various combinations of different end conditions. The discretized governing equations, subject to the motion-dependent force, are then obtained as

$$\ddot{\zeta}_m + b_m\dot{\eta}_m + [k_{m1} - 2\varepsilon(C\alpha_1^*/\alpha_m^*)\cos(\Omega_m t^*)]\zeta_m + 2\varepsilon(C\alpha_1^*/\alpha_m^*) \times \sum_{n=1, n\neq m}^{N} \{\cos[((\beta_m^* - \beta_n^*)/2\beta_m^*)\Omega_m t^*] - \cos[((\beta_m^* + \beta_n^*)/2\beta_m^*)\Omega_m t^*]\}\zeta_n$$

$$= (\sqrt{2}P_y^*/\alpha_m^*)\sin(\tfrac{1}{2}\Omega_m t^*), \qquad \ddot{\eta}_m - b_m\dot{\zeta}_m + k_{m2}\eta_m = (\sqrt{2}P_z^*/\alpha_m^*)\sin(\tfrac{1}{2}\Omega_m t^*), \tag{6}$$

where the parameters are defined as $\alpha_m^* = 1 + r^{*2}\beta_m^{*2}$, $b_m = 2\Omega^* r^{*2}\beta_1^{*2}\beta_m^{*2}/\alpha_m^*$, $k_{m2} = (\beta_m^{*4} - \Omega^{*2}r^{*2}\beta_1^{*4}\beta_m^{*2})/\alpha_m^*$, $k_{m1} = k_{m2} + 2\varepsilon C\alpha_1^*/\alpha_m^*$, $\varepsilon = \gamma/2C\alpha_1^* \ll 1$, C being a dummy constant for maintaining a small ε, and $\Omega_m = (2/\pi)\beta_1^{*2}\beta_m^* v^*$ is the excitation frequency of the mth mode due to the moving force.

3. STABILITY ANALYSIS

The method of multiple scales [13] is used here for analysis of the stability of the rotating beam. The non-homogeneous terms in the equations affect the solution but they have no effect on the stability of the solution of the linear equations (6). Therefore, those terms are omitted in the following stability analysis.

According to the method, the homogeneous solutions of equations (6) are expanded as

$$\zeta_m = \zeta_{m(0)}(T_0, T_1, \ldots) + \varepsilon\zeta_{m(1)}(T_0, T_1, \ldots) + \cdots,$$

$$\eta_m = \eta_{m(0)}(T_0, T_1, \ldots) + \varepsilon\eta_{m(1)}(T_0, T_1, \ldots) + \cdots, \tag{7}$$

where $T_n = \varepsilon^n t_1$ ($n = 0, 1, 2, \ldots$) denote time variables of different time scales. Substitution of the expanded solution (7) into the discretized equations and collecting coefficients of different powers of ε yields, to order ε^0,

$$D_0^2\zeta_{m(0)} + b_m D_0\eta_{m(0)} + k_{m1}\zeta_{m(0)} = 0, \qquad D_0^2\zeta_{m(0)} - b_m D_0\eta_{m(0)} + k_{m2}\eta_{m(0)} = 0, \tag{8}$$

and to order ε^1,

$$D_0^2\zeta_{m(1)} + b_m D_0\eta_{m(1)} + k_{m1}\zeta_{m(1)} = -2D_0D_1\zeta_{m(0)} - b_m D_1\eta_{m(0)} + 2(C\alpha_1^*/\alpha_m^*)\cos(\Omega_m T_0)\zeta_{m(0)}$$

$$+ 2(C\alpha_1^*/\alpha_m^*)\sum_{n=1, n\neq m}^{N}\left[\cos\left(\frac{\beta_m^* + \beta_n^*}{2\beta_m^*}\Omega_m T_0\right) - \cos\left(\frac{\beta_m^* - \beta_n^*}{2\beta_m^*}\Omega_m T_0\right)\right]\zeta_{n(0)},$$

$$D_0^2\eta_{m(1)} - b_m D_0\zeta_{m(1)} + k_{m2}\eta_{m(1)} = -2D_0D_1\eta_{m(0)} + b_m D_1\zeta_{m(0)} \tag{9}$$

where the differential operator D_i is defined as $D_i = \partial/\partial T_i$.

The eigenvalues of equations (8), ω_{m1} and ω_{m2}, are called the resonance frequencies of the mth mode, with $\omega_{m2} > \omega_{m1}$. Note that these resonance frequencies are exactly the natural frequencies of the rotating beam if one lets $\varepsilon = 0$. The general solution of equations (8) is thus of the form

$$\zeta_{m(0)} = A_{m1}\exp(\mathrm{i}\omega_{m1}T_0) + A_{m2}\exp(\mathrm{i}\omega_{m2}T_0) + \text{c.c.},$$

$$\eta_{m(0)} = \frac{\mathrm{i}(k_{m1}-\omega_{m1}^2)}{b_m\omega_{m1}}A_{m1}\exp(\mathrm{i}\omega_{m1}T_0) + \frac{\mathrm{i}(k_{m1}-\omega_{m2}^2)}{b_m\omega_{m2}}A_{m2}\exp(\mathrm{i}\omega_{m2}T_0) + \text{c.c.}, \tag{10}$$

where c.c. represents the corresponding complex conjugate terms, and A_{m1}, A_{m2} are complex functions of T_1, $T_2, \ldots$. Thus, equations (9) can be rewritten as

$$\begin{aligned}
&D_0^2\zeta_{m(1)} + b_m D_0\eta_{m(1)} + k_{m1}\zeta_{m(1)} \\
&\quad = -\frac{\mathrm{i}(k_{m1}+\omega_{m1}^2)}{\omega_{m1}}A'_{m1}\exp(\mathrm{i}\omega_{m1}T_0) - \frac{\mathrm{i}(k_{m1}+\omega_{m2}^2)}{\omega_{m2}}A'_{m2}\exp(\mathrm{i}\omega_{m2}T_0) \\
&\qquad + C\alpha_1^*/\alpha_m^*\{A_{m1}\exp[\mathrm{i}(\Omega_m+\omega_{m1})T_0] + \bar{A}_{m1}\exp[\mathrm{i}(\Omega_m-\omega_{m1})T_0] \\
&\qquad + A_{m2}\exp[\mathrm{i}(\Omega_m+\omega_{m2})T_0] + \bar{A}_{m2}\exp[\mathrm{i}(\Omega_m-\omega_{m2})T_0]\} \\
&\qquad + \frac{C\alpha_1^*}{\alpha_m^*}\sum_{n=1,n\neq m}^{N}\left\{A_{n1}\left[\exp\left(\mathrm{i}\left(\frac{\beta_m^*+\beta_n^*}{2\beta_m^*}\Omega_m+\omega_{n1}\right)T_0\right)\right.\right. \\
&\qquad \left.\left. - \exp\left(\mathrm{i}\left(\frac{\beta_m^*-\beta_n^*}{2\beta_m^*}\Omega_m+\omega_{n1}\right)T_0\right)\right] \\
&\qquad + \bar{A}_{n1}\left[\exp\left(\mathrm{i}\left(\frac{\beta_m^*+\beta_n^*}{2\beta_m^*}\Omega_m-\omega_{n1}\right)T_0\right) - \exp\left(\mathrm{i}\left(\frac{\beta_m^*-\beta_n^*}{2\beta_m^*}\Omega_m-\omega_{n1}\right)T_0\right)\right] \\
&\qquad + A_{n2}\left[\exp\left(\mathrm{i}\left(\frac{\beta_m^*+\beta_n^*}{2\beta_m^*}\Omega_m+\omega_{n2}\right)T_0\right) - \exp\left(\mathrm{i}\left(\frac{\beta_m^*-\beta_n^*}{2\beta_m^*}\Omega_m+\omega_{n2}\right)T_0\right)\right] \\
&\qquad + \bar{A}_{n2}\left[\exp\left(\mathrm{i}\left(\frac{\beta_m^*+\beta_n^*}{2\beta_m^*}\Omega_m-\omega_{n2}\right)T_0\right) - \exp\left(\mathrm{i}\left(\frac{\beta_m^*-\beta_n^*}{2\beta_m^*}\Omega_m-\omega_{n2}\right)T_0\right)\right] + \text{c.c.}, \\
&D_0^2\eta_{m(1)} - b_m D_0\zeta_{m(1)} + k_{m2}\eta_{m(1)} \\
&\quad = \frac{2k_{m1}+b_m^2-2\omega_{m1}^2}{b_m}A'_{m1}\exp(\mathrm{i}\omega_{m1}T_0) + \frac{2k_{m1}+b_m^2-2\omega_{m2}^2}{b_m}A'_{m2}\exp(\mathrm{i}\omega_{m2}T_0) + \text{c.c.},
\end{aligned} \tag{11}$$

in which the superscript $'$ denotes a derivative with respect to T_1 and $^-$ denotes the complex conjugate. Consider the equations of the mth mode only. The possible unstable conditions, can be seen by inspection of the right sides of equations (9), are found to be

$$\Omega_m \approx 2\omega_{m1}, \qquad \Omega_m \approx 2\omega_{m2}, \qquad \Omega_m \approx \omega_{m1}+\omega_{m2}, \qquad \Omega_m \approx \omega_{m2}-\omega_{m1}. \tag{12}$$

The first two cases are the so-called superharmonic resonances and the others are combination resonances. There would be an additional 16 possible instability conditions for each combination of m,n if the coupling effects of two different modes were taken into account. These conditions are

$$\begin{aligned}
&(\beta_m^* \pm \beta_n^*/2\beta_m^*)\Omega_m \approx \omega_{m1} \pm \omega_{n1}, \qquad (\beta_m^* \pm \beta_n^*/2\beta_m^*)\Omega_m \approx \omega_{m1} \pm \omega_{n2}, \\
&(\beta_m^* \pm \beta_n^*/2\beta_m^*)\Omega_m \approx \omega_{m2} \pm \omega_{n1}, \qquad (\beta_m^* \pm \beta_n^*/2\beta_m^*)\Omega_m \approx \omega_{m2} \pm \omega_{n2}.
\end{aligned} \tag{13}$$

The non-resonant and resonant cases are now discussed.

(a) No resonance. The system is in the non-resonant condition if none of the relations (12) and (13) occurs. Part of the non-homogeneous terms, in the right sides of equation (11), are of frequencies ω_{m1}, or ω_{m2}. They may induce an unstable response of the system. The unstable solution can be expressed as

$$\zeta_{m(1)} = P_{m1}\exp(\mathrm{i}\omega_{m1}T_0) + P_{m2}\exp(\mathrm{i}\omega_{m2}T_0) + \text{c.c.},$$
$$\eta_{m(1)} = Q_{m1}\exp(\mathrm{i}\omega_{m1}T_0) + Q_{m2}\exp(\mathrm{i}\omega_{m2}T_0) + \text{c.c.}, \tag{14}$$

where P_{m1}, P_{m2}, Q_{m1}, and Q_{m2} are complex functions of T_1, T_2, ... Substituting expressions (14) into equations (11) and equating coefficients of $\exp(\mathrm{i}\omega_{m1}T_0)$ and $\exp(\mathrm{i}\omega_{m2}T_0)$ on both sides, one obtains

$$(k_{m1} - \omega_{m1}^2)P_{m1} + \mathrm{i}\omega_{m1}b_mQ_{m1} = R_{m1}, \qquad -\mathrm{i}\omega_{m1}b_mP_{m1} + (k_{m2} - \omega_{m2}^1)Q_{m1} = R_{m2}, \tag{15}$$

$$(k_{m1} - \omega_{m2}^2)P_{m2} + \mathrm{i}\omega_{m2}b_mQ_{m2} = S_{m1}, \qquad -\mathrm{i}\omega_{m2}b_mP_{m2} + (k_{m2} - \omega_{m2}^2)Q_{m2} = S_{m2}, \tag{16}$$

with

$$R_{m1} = -(\mathrm{i}(k_{m1} + \omega_{m1}^2)/\omega_{m1})A'_{m1}, \qquad R_{m2} = [(2k_{m1} + b_m^2 - 2\omega_{m1}^2)/b_m]A'_{m1}, \tag{17}$$

$$S_{m1} = -(\mathrm{i}(k_{m1} + \omega_{m2}^2)/\omega_{m2})A'_{m2}, \qquad S_{m2} = [(2k_{m1} + b_m - 2\omega_{m2}^2)/b_m]A'_{m2}. \tag{18}$$

The conditions

$$\begin{vmatrix} k_{m1} - \omega_{m1}^2 & R_{m1} \\ -\mathrm{i}\omega_{m1}b_m & R_{m2} \end{vmatrix} = 0 \qquad \text{and} \qquad \begin{vmatrix} k_{m1} - \omega_{m2}^2 & S_{m1} \\ -\mathrm{i}\omega_{m2}b_m & S_{m2} \end{vmatrix} = 0 \tag{19, 20}$$

are required for non-trivial solutions of equations (15) and (16). As a consequence, one has

$$A'_{m1} = 0 \qquad \text{and} \qquad A'_{m2} = 0, \tag{21}$$

which imply that A_{m1}, A_{m2} are not functions of T_1. In other words, these two amplitudes can never go divergent; and consequently, no unstable response can be found. Therefore, the dynamic system in the non-resonant case is always stable.

(b) $\Omega_m \approx 2\omega_{m1}$. When Ω_m is close to $2\omega_{m1}$, let

$$\Omega_m = 2\omega_{m1} + \varepsilon\sigma \tag{22}$$

where σ is called the detuning parameter. One has

$$\exp[\mathrm{i}(\Omega_m - \omega_{m1})T_0] = \exp(\mathrm{i}\sigma T_1)\exp(\mathrm{i}\omega_{m1}T_0), \tag{23}$$

and, for this case, only part of the solution of frequency ω_{m1} needs to be considered. The analysis of equation (15), with different R_{m1} and R_{m2} from those in case (a), consequently gives the equation of the instability boundaries as

$$\Omega_m = 2\omega_{m1} \pm 2\varepsilon\Gamma_{m1} + O(\varepsilon^2), \tag{24}$$

or

$$v^* = [\pi/(2\beta_1^{*2}\beta_m^*)](2\omega_{m1} \pm 2\varepsilon\Gamma_{m1}) + O(\varepsilon^2), \tag{25}$$

with

$$\Gamma_{m1} = \tfrac{1}{2}[(k_{m1} - \omega_{m1}^2)^2/b_m + k_{m1}b_m]^{-1}C\alpha_1^*b_m\omega_{m1}/\alpha_m^*.$$

(c) $\Omega_m \approx 2\omega_{m2}$. For this case, let

$$\Omega_m = 2\omega_{m2} + \varepsilon\sigma \tag{26}$$

and consider the portion of the solution of frequency ω_{m2}. The instability boundaries are obtained as

$$v^* = [\pi/(2\beta_1^{*2}\beta_m^*)](2\omega_{m2} \pm 2\varepsilon\Gamma_{m2}) + O(\varepsilon^2) \tag{27}$$

with

$$\Gamma_{m2} = \tfrac{1}{2}[(k_{m1} - \omega_{m2}^2)^2/b_m + k_{m1}b_m]^{-1}C\alpha_1^* b_m\omega_{m2}/\alpha_m^*.$$

(d) $\Omega_m \approx \omega_{m1} + \omega_{m2}$. Define

$$\Omega_m = \omega_{m1} + \omega_{m2} + \varepsilon\sigma. \tag{28}$$

Two sets of equations are obtained, similar to equations (15) and (16), but with

$$R_{m1} = -\frac{\mathrm{i}(k_{m1} + \omega_{m1}^2)}{\omega_{m1}} A'_{m1} + (C\alpha_1^*/\alpha_m^*)\bar{A}_{m2}\exp(\mathrm{i}\sigma T_1),$$

$$R_{m2} = \frac{2k_{m1} + b_m^2 - 2\omega_{m1}^2}{b_m} A'_{m1}, \tag{29}$$

$$S_{m1} = -\frac{\mathrm{i}(k_{m1} + \omega_{m2}^2)}{\omega_{m2}} A'_{m2} + (C\alpha_1^*/\alpha_m^*)\bar{A}_{m1}\exp(\mathrm{i}\sigma T_1),$$

$$S_{m2} = \frac{2k_{m1} + b_m^2 - 2\omega_{m2}^2}{b_m} A'_{m2}. \tag{30}$$

Using equations (19) and (20) yields

$$A'_{m1} = \Gamma_{m1}\bar{A}_{m2}\exp(\mathrm{i}\sigma T_1 + \mathrm{i}\pi/2); \qquad A'_{m2} = \Gamma_{m2}\bar{A}_{m1}\exp(\mathrm{i}\sigma T_1 + \mathrm{i}\pi/2). \tag{31}$$

The solution of equations (31) is of the form

$$A_{m1} = (a_{1r} + \mathrm{i}a_{1i})\exp[\xi T_1 + \tfrac{1}{2}\mathrm{i}(\sigma T_1 + \pi/2)],$$

$$A_{m2} = (a_{2r} + \mathrm{i}a_{2i})\exp[\xi T_1 + \tfrac{1}{2}\mathrm{i}(\sigma T_1 + \pi/2)], \tag{32}$$

in which a_{1r}, a_{1i}, a_{2r}, and a_{2i} are real functions of T_2, T_3, . . . , and ξ is a real constant. For non-trivial A_{m1} and A_{m2}, the condition

$$\xi = \pm\sqrt{\Gamma_{m1}\Gamma_{m2} - (\sigma/2)^2} \tag{33}$$

must be satisfied. If $\Gamma_{m1}\Gamma_{m2} < (\sigma/2)^2$, the solution of the system is stable. The equation of the instability boundary is then written as

$$v^* = [\pi/(2\beta_1^{*2}\beta_m^*)](\omega_{m1} + \omega_{m2} \pm 2\varepsilon\sqrt{\Gamma_{m1}\Gamma_{m2}}) + O(\varepsilon^2). \tag{34}$$

(e) $\Omega_m \approx \omega_{m2} - \omega_{m1}$. The calculation is much the same as that for case (d) and it shows no instability when $\Omega_m \approx \omega_{m2} - \omega_{m1}$.

(f) $[(\beta_m^* \pm \beta_n^*)/(2\beta_m^*)]\Omega_m \approx \omega_{mp} + \omega_{nq}(p, q = 1, 2)$. In the present and next cases, consider two sets of discretized equations with mode numbers m and n. Through a procedure similar to that for case (a) but with more complicated calculations; the instability boundaries are found to be

$$v^* = \{\pi/[2\beta_1^{*2}(\beta_m^* \pm \beta_n^*)]\}(\omega_{mp} + \omega_{nq} + 2\varepsilon\sqrt{\Gamma_{mp}\Gamma_{nq}}) + O(\varepsilon^2). \tag{35}$$

(g) $[(\beta_m^* \pm \beta_n^*)/(2\beta_m^*)]\Gamma_m \approx \omega_{mp} - \omega_{nq}$ $(p, q = 1, 2)$. No instability occurs in these cases.

Analysis of the method of order higher than one, which is omitted here, can be performed by following similar processes but with much more work. Nevertheless, the possible instability conditions of order ε^2 and mode m can be obtained with less effort. They are

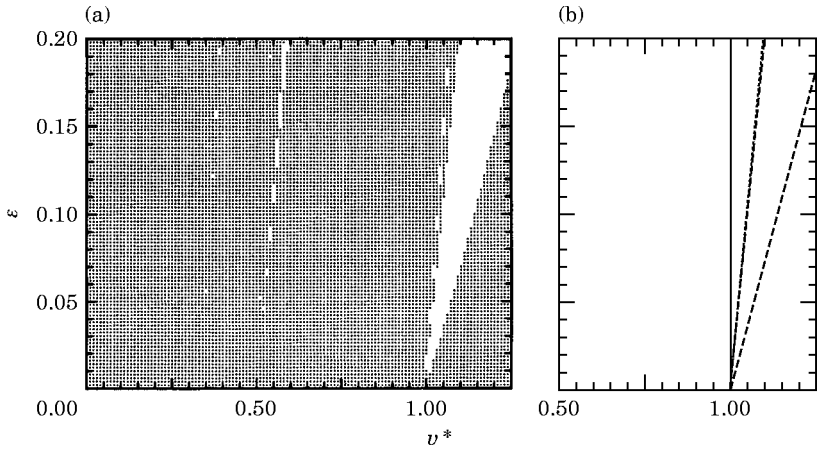

Figure 2. Instability regions for $m = 1$, $r^* = 0{\cdot}0125$ and $\Omega^*/\Omega^*_{cr} = 0{\cdot}10$. (a) From the numerical method; (b) from the method of multiple scales. ——, $\Omega_1 \approx 2\omega_{11}$; · · · · , $\Omega_1 \approx \omega_{11} + \omega_{12}$; — —, $\Omega_1 \approx 2\omega_{12}$.

$\Omega_m \approx \omega_{m1}$, ω_{m2}, $(\omega_{m1} + \omega_{m2})/2$ and $(\omega_{m2} - \omega_{m1})/2$. These frequencies are exactly half of the instability frequencies given in equations (12).

4. NUMERICAL RESULTS AND DISCUSSIONS

The stability of the time response of a rotating beam subject to the motion-dependent moving force is discussed next. The constant part of the external force is taken to be $P^*_y = P^*_z = 10$, and the dummy constant $C = 100$. Note that the amplitude of the motion-dependent force and the stability of the solution are dependent on γ and not on the choice of C. The value of γ can be obtained after ε and C are known. First, consider only the instabilities for the first mode ($m = 1$). Figures 2, 3 and 4 illustrate the instability regions for $r^* = 0{\cdot}0125$ and various frequencies of rotation. The abscissa denotes the dimensionless speed v^* of the external force, and the ordinate ε is proportional to the magnitude of the motion-dependent force. The results obtained by numerical integration in conjunction with the Floquet theory are given in parts (a), and those obtained by the method of multiple scales are shown in parts (b). The dotted areas given in (a) are stable regions found by the numerical method and the white areas are the unstable regions. In parts (b), the area between two solid lines is the unstable region near $\Omega_1 \approx 2\omega_{11}$, the area between two dotted lines is that near $\Omega_1 \approx \omega_{12} + \omega_{11}$, and the area within two dashed lines is that close to $\Omega_1 \approx 2\omega_{12}$. No instability occurs, as mentioned before, when $\Omega_1 \approx \omega_{12} - \omega_{11}$.

The stability of the solution for $\Omega^*/\Omega^*_{cr} = 0{\cdot}1$ is given in Figure 2. Here Ω^*_{cr} is defined as the smallest critical frequency of rotation and one has $\Omega^*_{cr} = 1/(\pi r^*)$ for a simply supported beam. The results obtained by the two different methods, as shown, agree very well. For a relatively low frequency of rotation, most of the unstable regions occur near $v^* = 1{\cdot}0$. The instability region near $\Omega_1 = 2\omega_{12}$ is quite large and merges with the small instability region close to $\Omega_1 = \omega_{11} + \omega_{12}$. On the other hand, the instability region near $\Omega_1 = 2\omega_{11}$ is too small to be found by the numerical method. Those instability boundaries look like straight lines for low frequencies of rotation. One can notice that in Figure 2(a) a narrow unstable region near $v^* = 0{\cdot}5$ exists. This region can be found analytically from the second order (ε^2) multiple scales analysis.

Figure 3 illustrates the instability boundaries for a medium rotational speed, $\Omega^*/\Omega^*_{cr} = 0{\cdot}65$. Satisfactory consistency between the results from two methods is seen. The

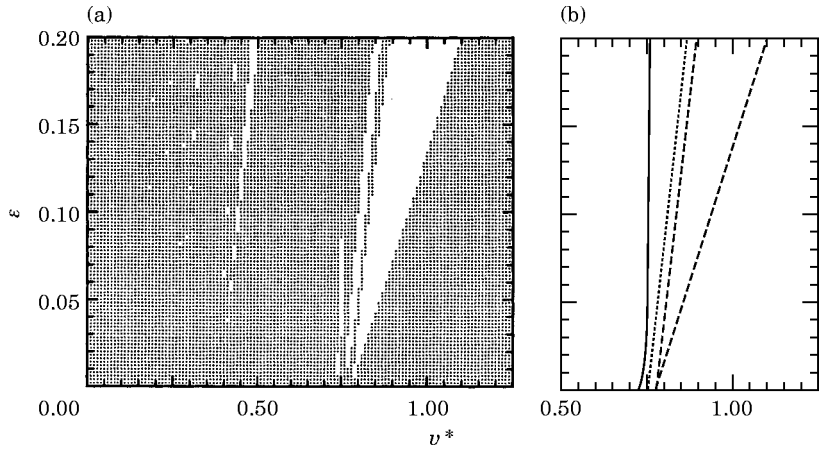

Figure 3. Instability regions for $m = 1$, $r^* = 0{\cdot}0125$ and $\Omega^*/\Omega^*_{cr} = 0{\cdot}65$. (a) From the numerical method; (b) from the method of multiple scales. ——, $\Omega_1 \approx 2\omega_{11}$; · · · · · , $\Omega_1 \approx \omega_{11} + \omega_{12}$; — —, $\Omega_1 \approx 2\omega_{12}$.

instabilities happen at comparatively lower force speeds than those for the smaller rotational frequency. As previously, numerical results shown some additional, small instability regions at low force speeds.

The instability regions for the case of $\Omega^*/\Omega^*_{cr} = 0{\cdot}99$ are presented in Figure 4. Since the rotational frequency is close to the critical one, numerous and complicated unstable regions were observed. All of the instabilities occur at low force speeds because the resonance frequencies of the rotating beam are small and the rotating beam itself has a tendency to instability. The instability boundaries become curves for a high rotational frequency. For the present case, the results given by the first order perturbation method seem not good enough to show all the instability regions. Some of the instability regions at low force speeds and corresponding to the high-order multiple scales method, look even wider than those of the first order.

The instability regions determined by the method of multiple scales, for $r^* = 0{\cdot}05$ and $\Omega^*/\Omega^*_{cr} = 0{\cdot}65$, are illustrated in Figure 5. The instability boundaries are similar to those in Figure 3(b) except found at larger force speeds.

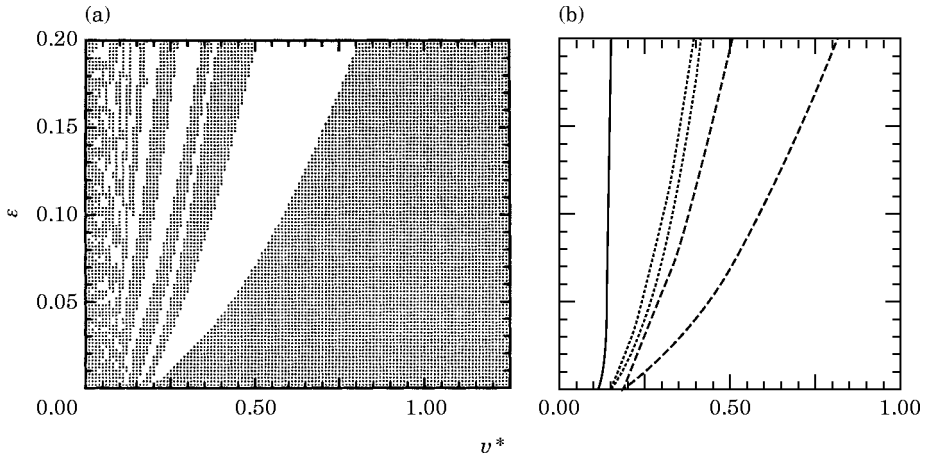

Figure 4. Instability regions for $m = 1$, $r^* = 0{\cdot}0125$ and $\Omega^*/\Omega^*_{cr} = 0{\cdot}99$. (a) From the numerical method; (b) from the method of multiple scales. ——, $\Omega_1 \approx 2\omega_{11}$; · · · · · , $\Omega_1 \approx \omega_{11} + \omega_{12}$; — —, $\Omega_1 \approx 2\omega_{12}$.

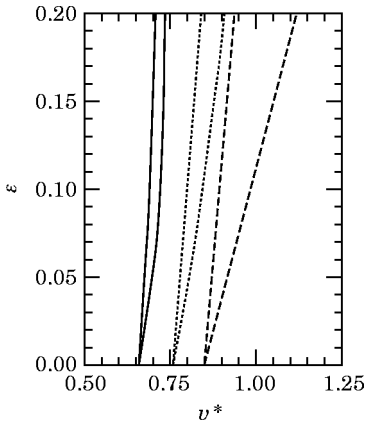

Figure 5. Instability regions for $m = 1$, $r^* = 0{\cdot}05$ and $\Omega^*/\Omega^*_{cr} = 0{\cdot}65$. ——, $\Omega_1 \approx 2\omega_{11}$; · · · · ·, $\Omega_1 \approx \omega_{11} + \omega_{12}$; — —, $\Omega_1 \approx 2\omega_{12}$.

The typical instability regions for the second mode ($m = 2$) are given in Figure 6. This figure is for the case of $r^* = 0{\cdot}0125$ and $\Omega^*/\Omega^*_{cr} = 0{\cdot}65$. All the instabilities occur near $v^* = 2$. These regions are much smaller than those of the first mode ($m = 1$) given in Figure 3(b).

To illustrate coupling effects of the first and the second modes ($m = 1, n = 2$), the instability regions for $r^* = 0{\cdot}0125$ and $\Omega^*/\Omega^*_{cr} = 0{\cdot}65$, are shown in Figure 7. The eight unstable regions, as derived in case (f) of the previous section, are divided into two groups. One group was found at force speeds close to $v^* = 1{\cdot}5$ and corresponds to the case of $\beta_1 + \beta_2$. The other was found at high force speeds near $v^* = 4{\cdot}5$ and corresponds to the case of $\beta_1 - \beta_2$. The instability regions in the second group are much larger then those in the first group, and are about the same size as those of the fundamental mode ($m = 1$). This phenomenon suggests that the instability due to the coupling between different vibration modes should not be neglected when the speed of the external force is large.

The unstable regions for higher modes ($m > 2$) and for other coupling modes, though not shown in the figures, were found to be quite small. These instabilities usually occur at high force speeds.

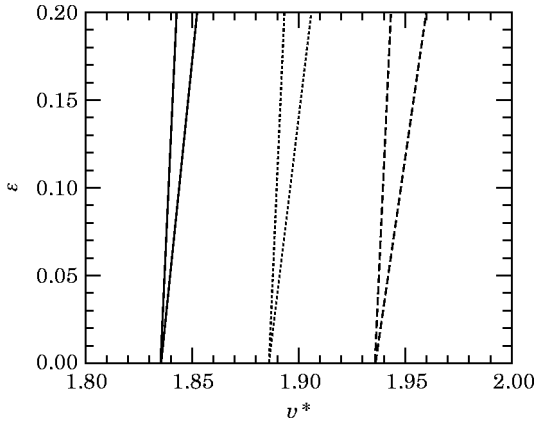

Figure 6. Instability regions for $m = 2$, $r^* = 0{\cdot}0125$ and $\Omega^*/\Omega^*_{cr} = 0{\cdot}65$. ——, $\Omega_2 \approx 2\omega_{21}$; · · · · ·, $\Omega_2 \approx \omega_{21} + \omega_{22}$; — —, $\Omega_2 \approx 2\omega_{22}$.

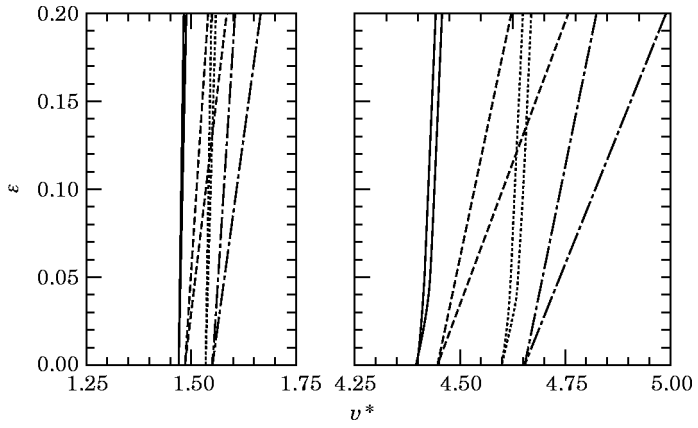

Figure 7. Instability regions for $m = 1$, $n = 2$, $r^* = 0{\cdot}0125$ and $\Omega^*/\Omega^*_{cr} = 0{\cdot}65$.

5. CONCLUSIONS

The stability of a rotating Rayleigh beam subject to a motion-dependent moving force has been discussed. The stability behavior was obtained via the method of multiple scales and verified by numerical methods. From the results, the following conclusions can be drawn.

1. The method of multiple scales can analytically predict the stability of the time response quite well provided that the rotational speed of the beam is not close to the critical rotational speed.

2. The largest instability region was found when the force speed related excitation frequency Ω_1 was nearly twice the higher resonance frequency ω_{12} of the first mode.

3. Coupling effects between the first two modes can result in large instability regions at high force speeds.

ACKNOWLEDGMENT

This work was sponsored by National Science Council, ROC, under the grant NSC 82-0422-E022-18; this support is gratefully acknowledged.

REFERENCES

1. J. T. Kenney, Jr. 1954 *Transactions of the ASME*, *Journal of Applied Mechanics*. **2**, 359–364. Steady-state vibrations of beam on elastic foundation for moving load.
2. A. L. Florence, 1965 *Transactions of the ASME*, *Journal of Applied Mechanics* **32**, 351–358. Traveling force on a Timoshenko beam.
3. R. Katz, C. W. Lee, A. G. Ulsoy and R. A. Scott 1987 *Transactions of the ASME*, *Journal of Vibration*, *Acoustics*, *Stress and Reliability in Design*, **109**, 361–365. Dynamic stability and response of a beam subject to a deflection dependent moving loading.
4. C. W. Lee, R. Katz, A. G. Ulsoy and R. A. Scott 1988 *Journal of Sound and Vibration* **122**, 119–130. Modal analysis of a distributed parameter rotating shaft.
5. R. Katz, C. W. Lee, A. G. Ulsoy and R. A. Scott 1988 *Journal of Sound and Vibration* **122**, 131–148. The dynamic response of a rotating shaft subject to a moving load.
6. S. C. Huang and J. S. Chen 1990 *Journal of the Chinese Society of Mechanical Engineers* **11**, 63–73. Dynamic response of spinning orthotropic beams subjected to moving harmonic forces.
7. A. Argento and R. A. Scott 1992 *Journal of Sound and Vibration* **157**, 221–231. Dynamic response of a rotating beam subjected to an accelerating distributed surface force.

8. A. Argento, H. L. Morano and R. A. Scott 1994 *ASME Journal of Vibration and Acoustics* **116**, 397–403. Accelerating load on a rotating Rayleigh beam.
9. A. Argento 1995 *Journal of Sound and Vibration* **182**, 595–615. A spinning beam subjected to a moving deflection dependent load, Part I: response and resonace.
10. A. Argento and H. L. Morano 1995 *Journal of Sound and Vibration* **182**, 617–622. A spinning beam subjected to a moving deflection dependent load, Part II: parametric resonance.
11. K. K. Chang 1993 *Master Thesis*, *National Central Universtiy*, *Chungli*, *Taiwan*, *R.O.C.* Dynamic behaviors of the workpiece in the lathing process.
12. Y. El-Karamany and F. Papai 1978 *International Journal of Machine Tool Design Research* **18**, 181–187. Determination of turning machine performance by nonlinear programming.
13. A. H. Nayfeh 1979 Nonlinear Oscillations. New York: Wiley.